Biosensors and Bioelectronics 292 (2026) 118061

Contents lists available at ScienceDirect

Biosensors and Bioelectronics

journal homepage: www.elsevier.com/locate/bios

Electrochemical biosensor for early Alzheimer's detection and patient risk stratification using plasma exosomes

Rosanna Rossi [a,b,*], Amanda Cano [c,d], Arnau Pallarès-Rusiñol [e], Agustín Ruiz [c,d,f], Merce Martí [a,g], Maria Isabel Pividori [a,b,**]

[a] Biosensing and Bioanalysis Group, Institute of Biotechnology and Biomedicine, Universitat Autònoma de Barcelona, Spain
[b] Grup de Sensors i Biosensors, Departament de Química, Universitat Autònoma de Barcelona, Bellaterra, Spain
[c] Research Center and Memory Clinic, Ace Alzheimer Center Barcelona, Barcelona, Spain
[d] Biomedical Research Networking Centre in Neurodegenerative Diseases (CIBERNED), Madrid, Spain
[e] BioEclosion SL, Avda. Can Domènech, Edifici Eureka, Universitat Autònoma de Barcelona, Bellaterra, Spain
[f] Glenn Biggs Institute for Alzheimer's & Neurodegenerative Diseases, The University of Texas at San Antonio, San Antonio, TX, USA
[g] Immunology Unit, Department of Cell Biology, Physiology, and Immunology, Institute of Biotechnology and Biomedicine, Universitat Autònoma de Barcelona, Bellaterra, Spain

ARTICLE INFO

Keywords:
Alzheimer's disease
Brain-derived exosomes
NLGN3
BACE-1
Electrochemical biosensor
Liquid biopsy

ABSTRACT

Alzheimer's Disease (AD) is the leading cause of dementia, accounting for 60–70 % of cases worldwide. Early diagnosis remains challenging due to the limitations of current diagnostic tools, which are costly, invasive, and suffer from low patient compliance. Blood-based biomarkers, particularly plasma brain-derived exosomes (BDEs), have emerged as a promising alternative since they carry AD-related molecules and can be isolated non-invasively. In this study, an immunoassay was developed to isolate BDEs using magnetic particles functionalized with an anti-neuroligin-3 (NLGN3) antibody, while the AD-related marker β-secretase (BACE-1) was detected on the captured exosomes. This is the first report combining NLGN3 for for the isolation of BDEs with BACE-1 as a detection target, establishing a novel biomarker panel for AD diagnostics. The assay was evaluated across three readout platforms—optical, chemiluminescent, and electrochemical—with detection limits in the range of 10^4–10^5 exosomes μL^{-1}. Among them, the portable electrochemical platform achieved the improved LOD (1.51×10^4 exosomes μL^{-1}, $R^2 = 0.9829$). Plasma samples from patients with AD, mild cognitive impairment (MCI), and healthy controls were analyzed, revealing differences in exosomal BACE-1 levels ($p < 0.1$, *t*-test). These findings demonstrate, for the first time, an *in vitro* diagnostic approach based on a portable electrochemical biosensor for early AD detection in plasma through a novel exosomal biomarker panel. Compared to conventional diagnostics, this biosensor offers a non-invasive and cost-effective solution for AD screening, with the potential to support earlier intervention and patient risk stratification.

1. Introduction

Alzheimer's disease (AD) represents the major form of dementia in the elderly. The main pathological hallmarks of AD are the oligomers and the aggregates of amyloid beta(Aβ) peptides, and intracellular deposits of hyperphosphorylated tau protein, known as neurofibrillary tangles (NFTs), which can be confirmed only analyzing the brain of the patient post-mortem. This is one of the reasons why it is so challenging to have the correct diagnosis of AD. Another reason is due to the long preclinical stage and prodromal period of this pathology, which can take up to 20 years (Vermunt et al., 2019). Also, dementia is usually a multifactorial condition that progresses through several stages, which further complicates both diagnosis and the decision process for clinicians. Unfortunately, there is no available disease-modifying therapy that could revert cognitive function in AD patients. However, therapies that slow disease progression are now emerging, with studies showing beneficial effects in early-diagnosed patients with mild symptoms. Consequently, there is growing consensus that the efficacy of disease-modifying treatments can only be demonstrated when initiated before the clinical onset of dementia. (Aisen et al., 2011). In this sense,

* Corresponding author. Biosensing and Bioanalysis Group, Institute of Biotechnology and Biomedicine, Universitat Autònoma de Barcelona, Spain.
** Corresponding author. Biosensing and Bioanalysis Group, Institute of Biotechnology and Biomedicine, Universitat Autònoma de Barcelona, Spain.
E-mail addresses: Rosanna.rossi@uab.cat (R. Rossi), Isabel.Pividori@uab.cat (M.I. Pividori).

https://doi.org/10.1016/j.bios.2025.118061
Received 27 August 2025; Received in revised form 22 September 2025; Accepted 1 October 2025
Available online 1 October 2025

an accurate and early diagnostic tool for AD is crucial. Current diagnostic techniques are based mainly on clinical examination and neuropsychological testing, such as Mini-Mental State Examination (MMSE), Montreal Cognitive Assessment (MoCA) and evaluation of clinical dementia rate (CDR). Clinical examination can be further supported by imaging techniques such as positron emission tomography (PET-amyloid, PET-tau, fluorodeoxyglucose-PET), magnetic resonance imaging (MRI) (Patel et al., 2020; Rowley et al., 2020; Valotassiou et al., 2018; Wei et al., 2016), as well as by biochemical analysis of cerebrospinal fluid (CSF) biomarkers (Ewers et al., 2015; Ma et al., 2022), often combined in the so-called AT(N) classification (Jack et al., 2016). However, current diagnostic tools have several limitations, especially in terms of costs, invasiveness and patient compliance. For these reasons, in most cases only patients that have already shown clinical manifestation of the symptoms are eligible for diagnosis. Also, in low-middle income countries the diagnostic gap for AD is even more pronounced, due to the limited economic resources. Therefore, in the last decade, an increasing effort has been focused on more accessible and easier diagnostic platforms using blood-based biomarkers for AD, particularly plasma p-tau isoforms (e.g., p-tau181, p-tau217, p-tau231) and neurofilament light chain (NfL), which have shown strong associations with amyloid and tau PET and are increasingly considered for clinical implementation (Ashton et al., 2024; Barthélemy et al., 2024; Khalil et al., 2018).

Exosomes are nano-sized extracellular vesicles (EVs) of endocytic origin, produced by most cell types (Gurung et al., 2021; Théry et al., 2018) in both physiological and pathologic conditions (Yates et al., 2022). In fact, as neuronal cells undergo changes associated with neurodegeneration, the molecular cargo of their exosomes mirrors these alterations (Cano et al., 2023a; Kalluri and LeBleu, 2020). There is evidence that AD alterations (synaptic dysfunction, β-amyloid accumulation, and Tau pathology) might be reflected in the number and composition of brain-derived exosomes, BDEs (Zhang et al., 2021; Cano et al., 2023b). In the context of AD, brain-derived exosomes (BDEs) are thought to play a dual and sometimes controversial role. On the one hand, they may contribute to disease progression by transporting and spreading toxic β-amyloid and pTau between cells (Hill, 2019), and by inducing apoptosis that exacerbates neuronal loss (Wang et al., 2012). On the other hand, exosomes have also been shown to facilitate β-amyloid clearance via microglial uptake and to transfer neuroprotective molecules between cells (Malm et al., 2016). While some mechanisms are still under investigation, there is clear evidence that exosomes originating from different regions of the brain can cross the blood–brain barrier (Banks et al., 2020) and are detectable in blood and other body fluids, making them highly promising candidates as clinical biomarkers (Soliman et al., 2021).

In this work, an innovative exosome-based biosensing platform for the detection and stratification of AD pathology is presented, evaluated through three complementary readout systems: optical, chemiluminescent, and electrochemical biosensing. In all formats, magnetic particles were functionalized with an anti-neuroligin-3 (NLGN3) antibody to selectively capture brain-derived exosomes (BDEs), while a biotinylated anti-β-secretase (BACE-1) antibody was used for detection. The combination of these two biomarkers is reported here for the first time and provides enhanced specificity compared to previous blood-based tests, which typically focus on a single protein biomarker such as plasma p-tau isoforms or neurofilament light (Ashton et al., 2024; Barthélemy et al., 2024; Khalil et al., 2018). While these soluble markers have shown strong clinical correlations, they are not exclusively brain-derived and may be affected by peripheral conditions. Also, although NfL is a robust indicator of axonal injury, its increase across various neurodegenerative disorders reduces its utility in distinguishing AD from other conditions (de Wolf et al., 2020). In contrast, the exosome-based approach ensures neuronal origin through NLGN3 capture and provides mechanistic insight into amyloidogenic processing via BACE-1 detection.

Importantly, the assay is also integrated into a portable electrochemical biosensor, successfully tested with plasma samples from AD and mild cognitive impairment (MCI) patients as well as healthy controls. Compared to imaging-based approaches (Patel et al., 2020; Rowley et al., 2020; Valotassiou et al., 2018; Wei et al., 2016) or lumbar puncture (Ewers et al., 2015), this platform offers a more accessible and patient-friendly diagnostic option. Furthermore, targeting neuronal-origin exosomes through NLGN3 increases the reliability of exosome isolation from plasma, addressing one of the key limitations in the field (Gurung et al., 2021; Théry et al., 2018). These preliminary results suggest that this approach may begin to address some of the limitations of current diagnostics and could support personalized medicine by capturing dynamic and individual-specific exosome profiles that reflect disease progression, treatment response, and subtype-specific characteristics (Yates et al., 2022). By coupling this selective capture with magnetic separation, the method also streamlines sample handling and facilitates integration into automated cartridges (Mathieu et al., 2019), supporting its translation into clinical workflows and large-scale AD screening.

2. Materials and methods

2.1. Instrumentation and chemical reagents

Nanoparticle tracking analysis (NTA) was conducted utilizing the NanoSight LM10-HS system (NanoSight Ltd, Malvern, GB). Cryogenic transmission electron microscopy (Cryo-TEM) images were acquired using a Jeol JEM 2011 (JEOL USA Inc, MA, US). Cytoflex LX equipment (Beckman Coulter Inc, Indianapolis, IN, US) was used for flow cytometry. Optical and chemiluminescent measurements were performed using a TECAN Infinite® M Plex (Tecan Group Ltd, Männeford, CH). The electrochemical signals were acquired using either a handheld potentiostat (BioEclosion SL, Bellaterra, ES) and a portable bipotentiostat (DRP-STAT200, DropSens, Metrohm AG, CH), operating on carbon screen-printed electrodes (ref. DRP-C110) placed within a disposable cartridge (BioEclosion SL, Bellaterra, ES) designed for magnetic actuation and electrochemical readout. Tosylactivated magnetic particles (MPs) (Dynabeads M450 Tosylactivated, ref. 14013), the Poly-HRP Streptavidin (Strep-polyHRP) (ref. 21140) and mouse monoclonal anti-NLGN3 (ref. MA527621), were purchased from Thermo Fisher Scientific (Waltham, MA, US). Biotinylated antibody anti-BACE-1 (ref. ABIN7145532) was obtained from Antibodies-online Inc. (Limerick, PA, US). Further details in instrumentation and reagents are provided in Supplementary Information (SI).

2.2. Cell culturing, exosome isolation and purification

Neuroblastoma SH-SY5Y cell lines were obtained from the American Type Culture Collection (ATCC) and used as a model of disease (Radagdam et al., 2023; Strother et al., 2021) for the production of BDEs to establish the method. Cell expansion was carried out using 5×10^6 cells in a T-175 flask containing 35 mL of DMEM/F12 medium, supplemented with 10 % exosome-depleted FBS and 100 U mL^{-1} penicillin-streptomycin. The culture was maintained at 37 °C in a humidified environment with 5 % CO_2. Once the cells reached approximately 90 % confluence in the T-175 flask, the culture supernatant was collected and stored at −20 °C for subsequent exosome isolation, following the protocol outlined in S2 and illustrated in Fig. S1 (SI).

2.3. Human samples collection and processing

Plasma samples from patients suffering from mild cognitive impairment (MCI), n = 5, and AD, n = 5, were obtained from Ace Alzheimer Center Barcelona as described elsewhere (Orellana et al., 2022). Briefly, patients were diagnosed and stratified by the AT(N) classification according to the National Institute on Aging and Alzheimer's Association. (Ebenau et al., 2020). The analyzed samples were anonymized and

pooled according to the previous criteria. All protocols have been approved by the ethics committee of the Ace Alzheimer Center Barcelona (approved in turn by the ethics committee of the Hospital Clinic, Barcelona, ES) in accordance with the Spanish Biomedicine Law and the declaration of Helsinki (World Medical Association, 2013). Informed consent for research on dementia was obtained from all participants prior to sample collection. Additionally, plasma samples from healthy donors, n = 50, were obtained from *Banc de Sang i Teixits*, Barcelona, pooled and used as negative control. All participant data from each cohort were stored pseudonymized. Pooled samples from each cohort, MCI, AD and Controls underwent differential ultracentrifugation for further characterization of the obtained exosomes. Detailed procedures are provided in S2 and S3 (SI).

2.4. Characterization of the exosomes derived from SH-SY5Y cell line and from plasma samples

The size, distribution, and concentration of purified exosomes were assessed using NTA, while their morphology was examined through Cryo-TEM. The total protein concentration in exosome samples was determined using a BCA protein assay kit. Detailed protocols are provided in S5.1 and S5.2 (SI). Additionally, flow cytometry analysis was performed on SH-SY5Y cells as described in S4 (SI) to identify potential surface biomarkers present on their derived exosomes, supporting the development of an exosome-based biosensing platform. The same biomarkers were then investigated on exosomes directly immobilized on magnetic particles (MPs), following the procedure described in S5.3 (SI). The biomarkers analyzed included CD9, CD63, CD81, BACE-1, NLGN3, L1CAM, GAP43, and Rab27b. Finally, MPs were functionalized with different capture antibodies (anti-CD81, anti-CD9, anti-L1CAM, anti-BACE-1, and anti-NLGN3), as described in S5.4 (SI), and the presence of these biomarkers was also assessed on exosomes previously captured with the modified MPs (S5.5, SI).

2.5. Capture efficiency of brain-derived exosomes on anti-NLGN3 magnetic particles

The ability of anti-NLGN3–functionalized magnetic particles to capture and preconcentrate BDEs was directly compared with anti-CD9–functionalized particles, which target the generic exosome marker CD9. The comparison was performed using SH-SY5Y-derived exosomes in a magneto-ELISA format with both optical and chemiluminescent readouts. Immobilization of antibodies anti-NLGN3 and anti-CD9 was conducted as described in S5.4 (SI). Exosomes were then captured using anti-NLGN3 or anti-CD9-modified MPs, with each well containing 1×10^6 anti-NLGN3-MPs or anti-CD9-MPs and 100 μL of exosomes at concentrations ranging from 2.0×10^4 to 4.4×10^7 exosomes μL^{-1}. The mixture was incubated for 1 h at 25 °C with gentle agitation. After incubation, the solution was discarded, and the wells were washed with 150 μL of PBS-BSA 0.5 % per well. Next, anti-CD63-HRP antibody (0.3 μg per well) diluted in PBS-BSA 0.1 % was added and incubated for 30 min at 25 °C, followed by four washes with PBS-BSA 0.5 %. Finally, for magneto-ELISA, 100 μL of Pierce™ TMB substrate solution were added to each well and incubated for 10 min at RT, and reaction was stopped by adding 100 μL of 2.0 mol L^{-1} H_2SO_4 for absorbance readout at 450 nm. In the case of chemiluminescence, 100 μL of SuperSignal™ ELISA Pico Chemiluminescent Substrate were added to each well and incubate for 1 min at RT for luminescent readout. Magnetic separation was performed after each incubation or washing step by placing a 96-well magnetic plate separator beneath the microtiter plate until the pellets formed in the lower corner, followed by the removal of the supernatant.

2.6. Magneto-actuated immunoassays for brain-derived exosomes using novel biomarkers NLGN3 and BACE-1

Once the performance of exosomes capture using anti-NLGN3-functionalized MPs was established, a comparative evaluation of magneto-actuated immunoassays for the specific detection of BDEs with optical, chemiluminescent and electrochemical readout was conducted. In this instance, exosomes were captured as described above. However, instead of employing a generic tetraspanin antibody for detection, a biotinylated anti-BACE-1 antibody (1.0 μg per well) was used to specifically detect BDEs. The antibody was incubated for 45 min at 25 °C. Following incubation and washing steps, streptavidin–poly-HRP was added and incubated for 30 min at 25 °C. Optical and chemiluminescent readout was performed as described in detail in S6 and S7 (SI), while electrochemical biosensing was performed as described in S8 (SI).

2.7. Electrochemical biosensor targeting brain-derived exosomes at different stages of AD

For the calibration plot, 100 μL of sample were incubated with 1×10^6 antiNLGN3-MPs for 1 h with gentle shaking at 25 °C. After incubation and washing, biotinylated anti-BACE-1 antibody (1.0 μg per assay) was then added and incubated for 45 min at 25 °C. The complex was incubated with streptavidin-poly-HRP (0.1 μg per assay) for 30 min at 25 °C. After washing, the content was transferred to a single-use microfluidic cartridge (BioEclosion SL) containing a screen-printed carbon electrode (DRP-C110, DropSens), in which the working and counter electrodes are carbon and the reference electrode is silver. The electrochemical measurement was performed by amperometry at −0.12 V (vs. Ag pseudo-reference) in a cartridge solution consisting of 100 mmol L^{-1} phosphate buffer with 100 mmol L^{-1} KCl (pH 7.0), supplemented with 2 mmol L^{-1} hydroquinone (HQ) as redox mediator and 2 mmol L^{-1} hydrogen peroxide (H_2O_2) as substrate. Under these conditions, the HRP enzyme catalyzes the HQ/BQ redox cycle, producing a cathodic current proportional to the amount of exosomes bound in the immunocomplex. A steady-state current was reached after ~30 s, and disposable electrodes and cartridges were discarded after each measurement. Further details related the electrochemical readout are provided in S8 (SI). To assess the analytical performance in human samples, exosomes isolated from the plasma of MCI and AD patients were used, while exosomes from healthy donor plasma served as the control.

2.8. Statistical analysis

GraphPad Prism 10 software (San Diego, CA, USA) was used to analyze the data, fitting all calibration curves that relate the concentration of exosomes to the analytical signal (absorbance, chemiluminescence, or current) by non-linear regression using the four-parameter logistic (4 PL) model. The limit of detection (LOD) was determined by measuring blank responses ($n \geq 4$), calculating their mean and standard deviation, and defining a threshold as the mean plus three standard deviations. This threshold was then interpolated on the calibration curves fitted with the four-parameter logistic (4 PL) model using GraphPad Prism 10, yielding the corresponding analyte concentration as the LOD.

3. Results and discussion

3.1. NTA and Cryo-TEM characterization of the exosomes derived from SH-SY5Y cell line and plasma samples

From NTA analysis, exosomes derived from SH-SY5Y cell lines showed a concentration of 1.59×10^{11} (SD 2.02×10^9) particles mL^{-1}. The size distribution histogram (Fig. 1A) displayed a primary peak at 155 nm and a secondary, broader peak at 225 nm, both consistent with the typical size range of exosomes (Théry et al., 2018). A similar size distribution across the three different pooled plasma samples was found, with a main peak at 135 nm for both extracellular vesicles (EVs) from healthy donors (Fig. 1B) and MCI patients (Fig. 1C), and a main peak at 125 nm followed by a second peak at 185 nm for EVs from AD patients

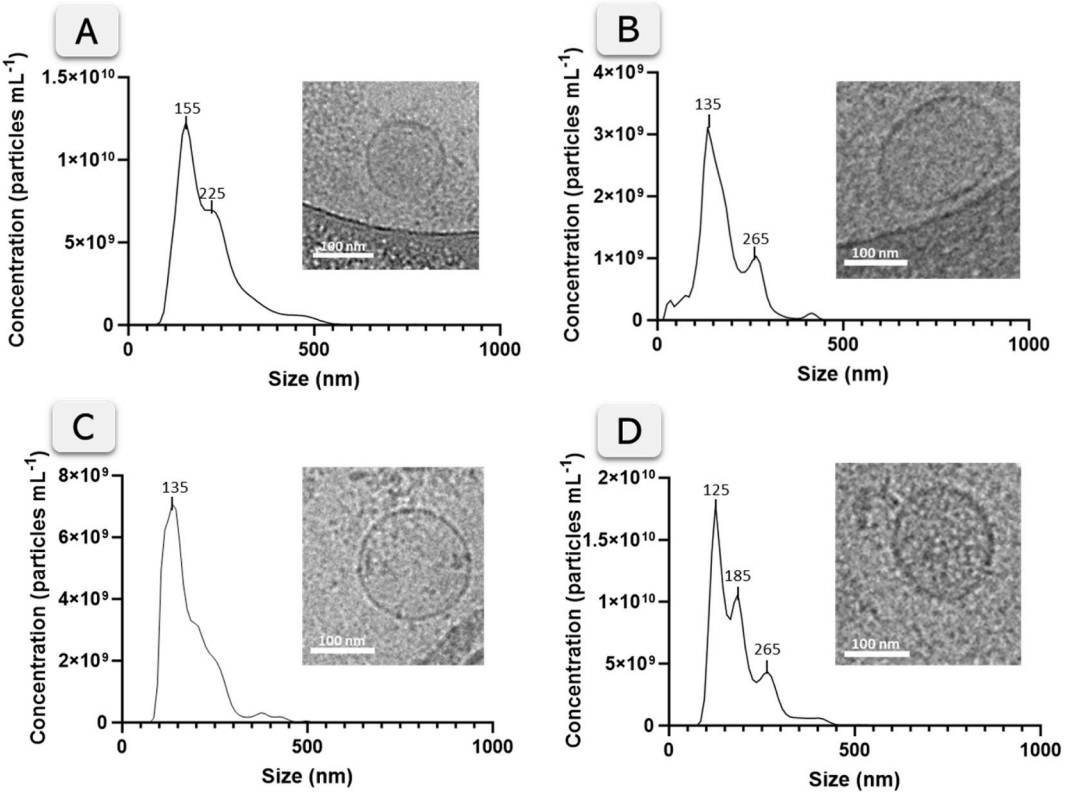

Fig. 1. Characterization of purified exosomes derived from SH-SY5Y cells (A), plasma of healthy donors (B), plasma from MCI patients (C), and plasma from AD patients (D) was conducted using NTA and Cryo-TEM. NTA analysis was performed by capturing raw data videos (n = 3), each lasting 60 s at a frame rate of 25 frames per second, with the laser unit temperature maintained at 24.8 °C. Cryo-TEM imaging was carried out at an acceleration voltage of 200 kV.

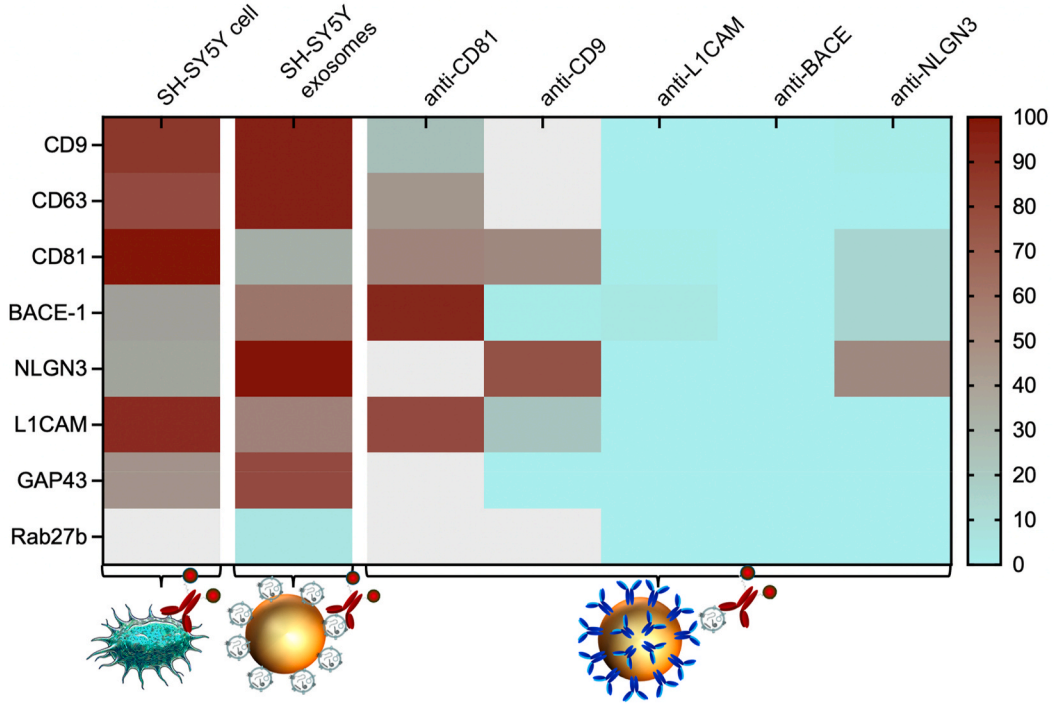

Fig. 2. Heatmap of bead-based flow cytometry. Column 1: SH-SY5Y cells; Column 2: exosomes directly immobilized on beads; Columns 3–7: exosomes captured with anti-CD81, anti-CD9, anti-L1CAM, anti-BACE-1 and anti-NLGN3, and detected with the antibody in each row. Color intensity indicates % positive events (red = high, cyan = low). For neuronal biomarkers in BDE, NLGN3 (capture) with biotinylated anti-BACE-1 (detection) showed the best performance (14.7 %). (For interpretation of the references to colour in this figure legend, the reader is referred to the Web version of this article.)

(Fig. 1D). All main peaks are compatible with exosomes size. Average concentration was respectively of 3.48×10^{10} (SD 1.44×10^{9}) particles mL^{-1} for EVs extracted from plasma of healthy donors, 7.64×10^{10} (SD 1.36×10^{9}) particles mL^{-1} for EVs extracted from plasma of MCI patients and 1.63×10^{11} (SD 6.43×10^{9}) particles mL^{-1} for EVs extracted from plasma of AD patients. Images extracted with Cryo-TEM also showed a particle's size compatible with exosomes, and confirmed vesicle integrity in all the cases, as shown as insets. Original Cryo-TEM pictures are shown in Fig. S3 (SI).

3.2. Flow cytometry characterization of the exosomes derived from SH-SY5Y cell line

Flow cytometry characterization of the exosomes derived from SH-SY5Y cells was performed to prove the presence of targeted molecules on SH-SY5Y cells membrane (as described in S4 and shown in Fig. S2, SI) and then select the best markers for the development of the exosome-based biosensing platform. The main findings are summarized as heatmap in Fig. 2. Initially, exosomes were directly immobilized on magnetic particles, and the presence of the tetraspanins CD9, CD63, and CD81 was assessed. These membrane proteins play a key role in maintaining protein structure and facilitating anchorage to cellular membranes. Due to their high expression in exosomes, tetraspanins CD9, CD63, and CD81 are commonly used as exosome universal biomarkers as they can influence exosome formation and composition (Hemler, 2003; Andreu and Yáñez-Mó, 2014; Théry et al., 2018). As shown in Fig. S4 (SI), SH-SY5Y exosome membrane was found particularly enriched in CD9 and CD63, with a positive labelling of 96.1 and 95.7 %, respectively, followed by CD81 at 36.8 %. Moreover, presence of possible neuronal and AD biomarkers was tested. In particular, attention was focused on NLGN3 as a potential neuronal marker to specifically capture BDEs. NLGN3 is a neuron cell surface marker localized at subsets of both excitatory and inhibitory synapses, regulating their functions (Uchigashima et al., 2020). The majority of previous studies on biomarkers in EVs used antibodies against L1CAM (L1 cell adhesion molecule, CD171) to capture BDEs (Fiandaca et al., 2015; Gomes and Witwer, 2022; Pulliam et al., 2019). However, although L1CAM is highly expressed at brain level, its expression by other cell types (as kidney, dermis, and peripheral lymphocytes, among others) is also remarkable ("The human protein Atlas," 2024a), raising concerns regarding BDEs origin and purity. On the other hand, NLGN3 is expressed exclusively at brain level, in particular from hippocampus ("The human protein Atlas," 2024b), which is one of brain areas firstly affected by AD, as the seat of the main neuronal connections involved in memory. This makes NLGN3 a particularly good candidate to pre-concentrate BDEs for early AD detection. Flow cytometry experiments showed that expression of NLGN3 on SH-SY5Y exosomes is remarkable and higher compared to that of L1CAM (Fig. S4, SI and heatmaps Fig. 2), being respectively 98.5 % and 59.1 %. Interestingly, expression of NLGN3 was higher on membrane of SH-SY5Y exosomes than on membrane of parental cells, while the opposite happens with L1CAM (Fig. S2 and S4, SI and heatmap Fig. 2). This observation suggests possible mechanisms of NLGN3 enrichment on the membrane of BDEs during exosome formation, highlighting this molecule as a particularly relevant target for BDE capture.

Further experiments involved the search for biomarkers specific for AD on the membrane of SH-SY5Y exosomes. Among these, several possible biomarkers for AD were considered, such as BACE-1, GAP-43 and Rab27b. BACE-1 is the β-secretase responsible for cleaving the transmembrane amyloid precursor protein (APP) and, together with γ-secretase, generates Aβ peptides in the amyloidogenic pathway. Aβ peptides are small peptides of 39–43 amino acids in length that represent the major content of amyloid deposits typical of AD (Bibl et al., 2012). BACE-1 is the rate-limiting enzyme in Aβ peptides production, and several studies correlated its increased activity with the development of AD (Bao et al., 2018; Hampel et al., 2021). Growth-associated protein 43 (GAP-43) is a presynaptic protein involved in the regulation of axonal outgrowth, synaptic plasticity, and learning and memory functions (Skene et al., 1986) and recent studies correlated its overexpression with AD (Remnestål et al., 2016; Sandelius et al., 2019). Rab27b is a GTPase from Ras-related proteins (RAB) family (Srikanth et al., 2017). Recent studies found that Rab proteins are implicated in the progression of non-communicable diseases such as cancer (Fan et al., 2024; Xu et al., 2024) as well as in promoting extracellular vesicle secretion (Blanc and Vidal, 2018). Specifically, Rab27b has been implicated in neurodegenerative disorders (Underwood et al., 2020) and there is evidence of its high expression in cholinergic basal forebrain neurons associated with cognitive decline in MCI and AD (Ginsberg et al., 2011). Flow cytometry experiments showed a high expression of GAP-43 on the membrane of exosomes (81.9 %) followed by BACE-1 (65.4 %) and finally by Rab27b (6.5 %) (Fig. S4, SI and Fig. 2).

Further flow cytometry experiments were performed to select the best pair of markers for the biosensor platform design by using both a capture and a detection antibody simultaneously, as described in S5.5 (SI). As expected, a general decrease in signal intensity is observed compared to single-marker detection, since only exosomes simultaneously carrying both biomarkers are targeted, resulting in a lower percentage of positive events. This effect is especially evident for the combinations involving AD-related markers together with BDE markers. Nevertheless, NLGN3 was confirmed as the most suitable option for the specific capture of BDEs, while biotinylated anti-BACE-1 was identified as the best detection antibody, yielding the lowest background and a positive labeling of 14.7 %. In the final biosensing system, the use of streptavidin–polyHRP will be critical to further amplify the signal.

3.3. Capture efficiency of brain-derived exosomes on anti-NLGN3 magnetic particles

Additional experiments were conducted using magnetic particles functionalized with antibodies against NLGN3, a neuronal-origin marker, and against CD9, a general tetraspanin highly expressed in BDEs, in order to comparatively evaluate their ability to capture, isolate, and concentrate exosomes. Detection was performed targeting the other highly expressed tetraspanin, CD63, with the labelled antibody antiCD63-HRP performing a magneto-immunoassay with optical (A) and chemiluminescent (B) readout (Fig. 3).

When antiNLGN3-MPs were used, the regression coefficients (R^2) of the fittings obtained by four parameters logistic (4 PL) equation were 0.9758 for the optical readout and 0.9979 for the chemiluminescent readout, indicating high fitting and reliability of the assays, with a LOD of 7.13×10^{6} exosomes and 7.83×10^{6} exosomes for optical and chemiluminescent readout, respectively. When antiCD9-MPs were used, the R^2 obtained by the 4 PL equation were 0.9805 and 0.9893 for the optical and chemiluminescent readout, respectively, indicating also high fittings and reliability of the assays. The LOD for antiCD9-MPs were 4.91×10^{6} and 6.92×10^{5} exosomes for optical and chemiluminescent readout, respectively. As CD9 is a generic exosome marker, a higher capture was obtained with antiCD9-MPs, with slightly lower LOD, especially for the chemiluminescent assay. However, both modified MPs showed good results with similar performances overall, across the two readout systems. Specifically, antiNLGN3-MPs showed good capture capabilities, with the advantage of capturing selectively brain derived exosomes.

A new magneto-actuated immunoassay was first validated using model BDEs obtained from the SH-SY5Y cell line. The assay uniquely combines NLGN3 as a neuronal capture marker with BACE-1 as a detection marker of AD. This innovative platform was evaluated with three complementary readout strategies—optical, chemiluminescent, and portable electrochemical biosensing—demonstrating for the first time the versatility of this dual-biomarker approach for exosome analysis. Fig. 4A illustrates the magnetic capture and detection scheme, while Fig. 4B presents the normalized calibration plots obtained with each readout.

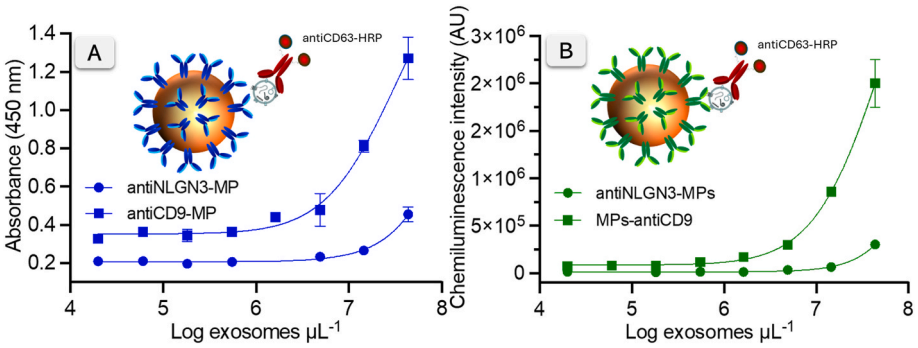

Fig. 3. Magneto-actuated immunoassays with optical (panel A) and chemiluminescent (panel B) readout to evaluate capture capabilities of antiNLGN3-MPs compared to antiCD9-MPs. Detection used antiCD63-HRP. Calibration plots used SH-SY5Y exosomes and are fitted with a non-linear regression model based on a four-parameter logistic equation. Bars show the SD of replicates (n = 3).

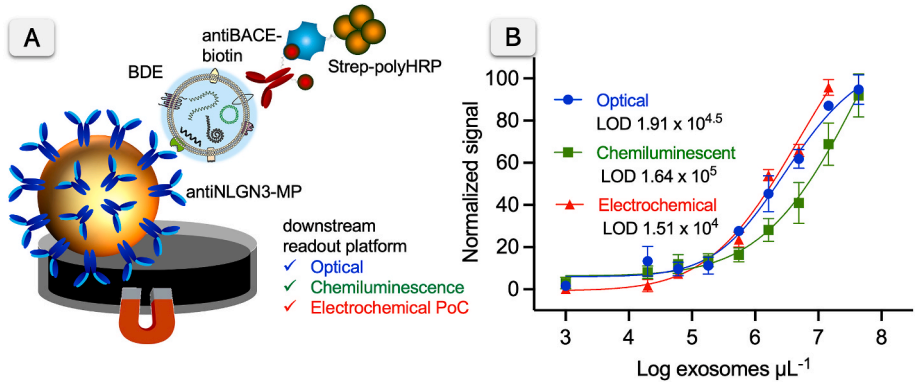

Fig. 4. (A) Schematic representation of the magneto-actuated immunoassay for AD-related biomarker detection in brain-derived exosomes (BDEs) using SH-SY5Y exosomes as a model. Magnetic particles functionalized with anti-NLGN3 antibody were employed to selectively capture BDEs, while detection was achieved with biotinylated anti-BACE-1 and streptavidin–poly-HRP (Strep-Poly-HRP) to amplify the signal. (B) Normalized calibration plots using optical (absorbance at 450 nm), chemiluminescent readouts, and electrochemical biosensing. LOD for each platform are indicated. Plots were fitted with a 4 PL model, and error bars represent the standard deviation of replicates (n = 3).

The calibration plots were constructed for different exosome concentrations, ranging from 2.03×10^4 to 4.4×10^7 exosomes μL^{-1} for the optical and the chemiluminescent readout and from 2.03×10^4 to 1.45×10^7 exosomes μL^{-1} for the electrochemical biosensor. In each case, the values were analyzed using a non-linear regression model based on a four-parameter logistic equation. The LODs were $1.91 \times 10^{4.5}$ exosomes μL^{-1} ($R^2 = 0.9791$), 1.64×10^5 exosomes μL^{-1} ($R^2 = 0.9598$), and 1.51×10^4 exosomes μL^{-1} ($R^2 = 0.9829$), respectively, for the magneto-actuated immunoassays with optical and chemiluminescent readout, and electrochemical biosensing. The three platforms gave overall comparable results, with a high fitting indicating that the assays were highly reliable and robust. However, the electrochemical biosensing resulted in a lower LOD and was selected to further analysis of plasma exosomes from patients with differential stages of cognitive impairment. The enhanced sensitivity of the electrochemical platform can be attributed to several factors. Firstly, electrochemical detection methods often exhibit higher sensitivity due to the amplification of the electrical signal produced by the redox reactions of the substrate at the electrode surface. Furthermore, electrochemical detection is less prone to interference from background noise compared to optical and chemiluminescent methods, which can be affected by variations in light absorption and scattering, resulting in a clearer and more distinct signal, and enhancing the sensitivity of the assay (Perju and Wongkaew, 2021). Overall, the LOD values are consistent with previous studies developing *in-vitro* diagnostic (IVD) test based on exosomes for other pathologies, such as breast cancer (Moura et al., 2020). However, to the best of our knowledge, this is the first IVD test based on brain-derived exosomes, enhancing the significance of the obtained results.

3.4. Electrochemical biosensor for the detection of brain derived exosomes in plasma

The analysis of exosomes from plasma of patients was carried out using a portable device operated by batteries integrated with a screen-printed electrode. Human sample analysis clearly showed the ability of the method to distinguish healthy subjects (Control) from the dementia group and, within this latter, to distinguish patients with MCI from AD patients (Fig. 5). Cathodic currents of 1.60 (SD 0.08) µA, 1.94 (SD 0.07) µA and 2.16 (SD 0.34) µA were recorded for control, MCI and AD, respectively, showed significant differences ($p < 0.1$, *t*-test). It should be noted that the reported standard deviations inherently reflect electrode-to-electrode variability, since each replicate was measured on a new disposable screen-printed electrode, thereby reinforcing the robustness of the observed differences across clinical groups. The statistical significance observed in this study ($p < 0.1$) is related to the limited number of samples analyzed and will need to be confirmed in larger patient cohorts.

These results are in line with the NTA results showing a progressively higher plasma concentration of exosomes from healthy subjects to MCI and AD patients (Fig. 1). This finding is supported by previous studies indicating both an increased exosome production from cells under stressed conditions (Ludwig et al., 2020), such as brain cells during neurodegenerative processes, and, specifically for AD, an additional increase in BACE-1 activity at the brain level (Cheng et al., 2014), which is compatible with an increased BACE-1 expression at the brain level and, possibly, at the level of BDEs. A higher presence of BDEs in the plasma of patients with neurodegenerative disorders could also be

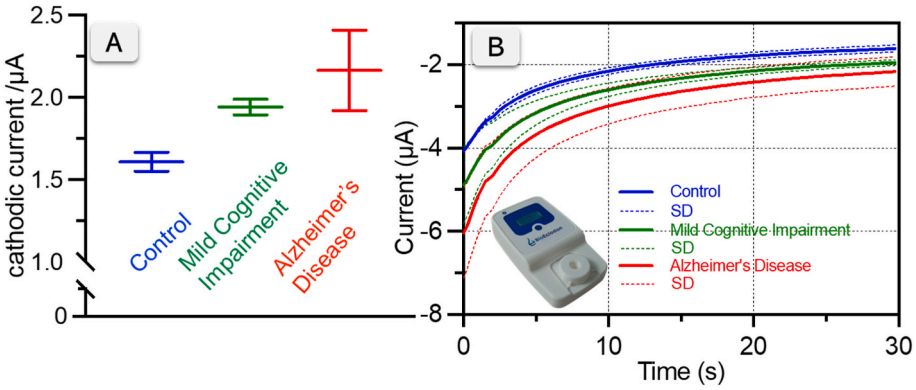

Fig. 5. Analysis of exosomes from pooled plasma of patients with MCI and AD compared to healthy subjects (Control), showing the platform's risk stratification capability. In all cases two replicate measurements were performed. (A) Bar plots and (B). Raw chronoamperograms of the samples measured with the hand-held electrochemical platform integrated with a screen-printed electrode and operated by batteries, adapted for use as IVD test.

explained by the progressive disruption of the BBB in these conditions (Sweeney et al., 2018), increasing its permeability for small lipophilic EVs such as exosomes. The stratification of patients in Fig. 5 is based on significant differences in exosomal BACE-1 levels, as measured using the hand-held portable electrochemical biosensor. These results indicate that the method is effective for distinguishing different stages of cognitive impairment, highlighting its potential as a diagnostic tool. The raw chronoamperograms (Fig. 5, panel B) further support this distinction, showing consistent trends in electrochemical signal variations among the groups. The significant differences between the groups suggest that exosomal BACE-1 levels correlate with disease progression, reinforcing the platform's capability for early AD detection and patient risk stratification.

4. Conclusions

This study presents a novel dual-biomarker strategy for the isolation and detection of brain-derived exosomes (BDEs) from plasma. By combining a neuronal marker (neuroligin-3, NLGN3) for exosome capture with an Alzheimer's-related enzyme (β-secretase 1, BACE-1) for detection, highly specific isolation of neuron-origin vesicles in a minimally invasive blood sample is achieved. Targeting two complementary biomarkers simultaneously provides richer information than single-marker approaches and has the potential to improve diagnostic accuracy and early detection of Alzheimer's disease.

The magneto-actuated immunoassay demonstrated compatibility with multiple analytical platforms, including optical, chemiluminescent, and electrochemical systems. The assay can be integrated into standard laboratory equipment or adapted to portable point-of-care devices such as screen-printed electrode platforms, making it suitable for both centralized laboratories and on-site screening applications. This versatility supports the potential for broader adoption in routine testing.

The selective targeting of neuron-derived exosomes in plasma is particularly relevant for Alzheimer's disease screening. Exosomes are present in all body fluids, and neuron-specific vesicles can be isolated from blood, providing a non-invasive means of assessing brain changes before the onset of clinical symptoms. Although isolating exosomes from plasma remains challenging due to their low abundance and the complexity of the matrix, the dual-marker strategy enhances specificity for disease-relevant vesicles and offers a promising approach for early risk assessment.

Future clinical validation in larger cohorts of individual samples will be required to confirm diagnostic performance, establish robustness, determine the potential of this platform for patient stratification and early Alzheimer's disease screening, and enable the calculation of ROC curves and sensitivity/specificity metrics that are essential to fully establish diagnostic accuracy and clinical applicability. These results should therefore be regarded as a preliminary proof-of-concept, as the analysis was performed on small pooled cohorts to minimize inter-individual variability, providing conceptual validation of the approach while highlighting the need for further confirmation in independent studies.

CRediT authorship contribution statement

Rosanna Rossi: Writing – original draft, Validation, Methodology, Investigation, Formal analysis. **Amanda Cano:** Resources, Methodology, Investigation, Data curation. **Arnau Pallarès-Rusiñol:** Methodology, Investigation. **Agustín Ruiz:** Supervision, Resources, Funding acquisition. **Merce Martí:** Validation, Supervision, Project administration, Investigation, Conceptualization. **Maria Isabel Pividori:** Writing – review & editing, Validation, Supervision, Resources, Project administration, Investigation, Funding acquisition, Conceptualization.

Declarations

All protocols of the current study have been approved by the Clinical Research Ethics Commission of the Hospital Clinic (Barcelona, Spain) in accordance with the current Spanish regulations in the field of biomedical research and the Declaration of Helsinki. Likewise, in accordance with Spain's Data Protection Law, all participants were informed about the study's goals and procedures by a neurologist before signing an informed consent form. Patients' privacy and data confidentiality were protected in accordance with applicable laws.

Declaration of competing interest

The authors declare that they have no known competing financial interests or personal relationships that could have appeared to influence the work reported in this paper.

Acknowledgment

This research was funded by the Ministry of Science, Innovation and Universities, Spain (Project PDC2022-133363-I00, Grant FPU16/01579, Grants Margarita Salas y María Zambrano and Subvencions de l'Ajuntament de Barcelona per a projectes de recerca jove i emergent 2024, Ref: 24S05876-001). Also, ICTS "NANBIOSIS" NTA analysis service of Institut de Ciència dels Materials de Barcelona, of Universitat Autònoma de Barcelona is gratefully acknowledged. Authors acknowledge the support of the Spanish Ministry of Science and Innovation, Proyectos de Generación de Conocimiento grant PID2021-122473OA-I00. The support of CIBERNED (ISCIII) under the grant CB18/05/00010. The support of Fundación ADEY, under the program "Proyectos de Investigación en

Salud 2023". A. Cano acknowledges the support of the Instituto de Salud Carlos III (ISCIII) under the grant Sara Borrell (CD22/00125).

Appendix A. Supplementary data

Supplementary data to this article can be found online at https://doi.org/10.1016/j.bios.2025.118061.

Data availability

Data will be made available on request.

References

Aisen, P.S., Andrieu, S., Sampaio, C., Carrillo, M., Khachaturian, Z.S., Dubois, B., Feldman, H.H., Petersen, R.C., Siemers, E., Doody, R.S., Hendrix, S.B., Grundman, M., Schneider, L.S., Schindler, R.J., Salmon, E., Potter, W.Z., Thomas, R. G., Salmon, D., Donohue, M., Bednar, M.M., Touchon, J., Vellas, B., 2011. Neurology 76, 280–286. https://doi.org/10.1212/WNL.0b013e318207b1b9.

Andreu, Z., Yáñez-Mó, M., 2014. Front. Immunol. 5. https://doi.org/10.3389/fimmu.2014.00442.

Ashton, N.J., Brum, W.S., Di Molfetta, G., Benedet, A.L., Arslan, B., Jonaitis, E., Langhough, R.E., Cody, K., Wilson, R., Carlsson, C.M., Vanmechelen, E., Montoliu-Gaya, L., Lantero-Rodriguez, J., Rahmouni, N., Tissot, C., Stevenson, J., Servaes, S., Therriault, J., Pascoal, T., Lleó, A., Alcolea, D., Fortea, J., Rosa-Neto, P., Johnson, S., Jeromin, A., Blennow, K., Zetterberg, H., 2024. JAMA Neurol. 81, 255. https://doi.org/10.1001/jamaneurol.2023.5319.

Banks, W.A., Sharma, P., Bullock, K.M., Hansen, K.M., Ludwig, N., Whiteside, T.L., 2020. Int. J. Mol. Sci. 21, 4407. https://doi.org/10.3390/ijms21124407.

Bao, J., Qin, M., Mahaman, Y.A.R., Zhang, B., Huang, F., Zeng, K., Xia, Y., Ke, D., Wang, Q., Liu, R., Wang, J.-Z., Ye, K., Wang, X., 2018. Proc. Natl. Acad. Sci. 115, 3954–3959. https://doi.org/10.1073/pnas.1800498115.

Barthélemy, N.R., Salvadó, G., Schindler, S.E., He, Y., Janelidze, S., Collij, L.E., Saef, B., Henson, R.L., Chen, C.D., Gordon, B.A., Li, Y., La Joie, R., Benzinger, T.L.S., Morris, J.C., Mattsson-Carlgren, N., Palmqvist, S., Ossenkoppele, R., Rabinovici, G. D., Stomrud, E., Bateman, R.J., Hansson, O., 2024. Nat. Med. 30, 1085–1095. https://doi.org/10.1038/s41591-024-02869-z.

Bibl, M., Esselmann, H., Wiltfang, J., 2012. Ther. Adv. Neurol. Disord. 5, 335–348. https://doi.org/10.1177/1756285612455367.

Blanc, L., Vidal, M., 2018. Small GTPases 9, 95–106. https://doi.org/10.1080/21541248.2016.1264352.

Cano, A., Ettcheto, M., Bernuz, M., Puerta, R., Esteban de Antonio, E., Sánchez-López, E., Souto, E.B., Camins, A., Martí, M., Pividori, M.I., Boada, M., Ruiz, A., 2023a. Int. J. Biol. Sci. 19, 721–743. https://doi.org/10.7150/ijbs.79063.

Cano, A., García, P., Bernuz, M., Puerta, R., de Rojas, I., Esteban-De Antonio, E., Pérez-Cordón, A., Montreal, L., Núñez, R., Sotolongo-Grau, Ó., Alonso-Lana, S., Alarcón-Martín, E., Valero, S., Alegret, M., Martínez, J., Martín, E., Ettcheto, M., Vivas, A., Gomez-Chiari, M., Tejero, M.A., Orellana, A., Tárraga, L., Marquié, M., Martí, M., Pividori, M.I., Boada, M., Ruiz, A., 2023b. J. Nanobiotechnol. 21, 1–19. https://doi.org/10.1186/s12951-023-01793-7.

Cheng, X., He, P., Lee, T., Yao, H., Li, R., Shen, Y., 2014. Am. J. Pathol. 184, 141–147. https://doi.org/10.1016/j.ajpath.2013.10.002.

de Wolf, F., Ghanbari, M., Licher, S., McRae-McKee, K., Gras, L., Weverling, G.J., Wermeling, P., Sedaghat, S., Ikram, M.K., Waziry, R., Koudstaal, W., Klap, J., Kostense, S., Hofman, A., Anderson, R., Goudsmit, J., Ikram, M.A., 2020. Brain 143, 1220–1232. https://doi.org/10.1093/brain/awaa054.

Ebenau, J.L., Timmers, T., Wesselman, L.M.P., Verberk, I.M.W., Verfaillie, S.C.J., Slot, R. E.R., van Harten, A.C., Teunissen, C.E., Barkhof, F., van den Bosch, K.A., van Leeuwenstijn, M., Tomassen, J., Braber, A. den, Visser, P.J., Prins, N.D., Sikkes, S.A. M., Scheltens, P., van Berckel, B.N.M., van der Flier, W.M., 2020. Neurology 95. https://doi.org/10.1212/WNL.0000000000009724.

Ewers, M., Mattsson, N., Minthon, L., Molinuevo, J.L., Antonell, A., Popp, J., Jessen, F., Herukka, S., Soininen, H., Maetzler, W., Leyhe, T., Bürger, K., Taniguchi, M., Urakami, K., Lista, S., Dubois, B., Blennow, K., Hampel, H., 2015. Alzheimer's Dement. 11, 1306–1315. https://doi.org/10.1016/j.jalz.2014.12.006.

Fan, B., Wang, L., Wang, J., 2024. Aging 16, 4169–4190. https://doi.org/10.18632/aging.205565.

Fiandaca, M.S., Kapogiannis, D., Mapstone, M., Boxer, A., Eitan, E., Schwartz, J.B., Abner, E.L., Petersen, R.C., Federoff, H.J., Miller, B.L., Goetzl, E.J., 2015. Alzheimer's Dement. 11, 600. https://doi.org/10.1016/j.jalz.2014.06.008.

Ginsberg, S.D., Mufson, E.J., Alldred, M.J., Counts, S.E., Wuu, J., Nixon, R.A., Che, S., 2011. J. Chem. Neuroanat. 42, 102–110. https://doi.org/10.1016/j.jchemneu.2011.05.012.

Gomes, D.E., Witwer, K.W., 2022. J. Extracell. Biol. 1. https://doi.org/10.1002/jex2.35.

Gurung, S., Perocheau, D., Touramanidou, L., Baruteau, J., 2021. Cell Commun. Signal. 19, 47. https://doi.org/10.1186/s12964-021-00730-1.

Hampel, H., Vassar, R., De Strooper, B., Hardy, J., Willem, M., Singh, N., Zhou, J., Yan, R., Vanmechelen, E., De Vos, A., Nisticò, R., Corbo, M., Imbimbo, B. Pietro, Streffer, J., Voytyuk, I., Timmers, M., Tahami Monfared, A.A., Irizarry, M., Albala, B., Koyama, A., Watanabe, N., Kimura, T., Yarenis, L., Lista, S., Kramer, L., Vergallo, A., 2021. Biol. Psychiatry 89, 745–756. https://doi.org/10.1016/j.biopsych.2020.02.001.

Hemler, M.E., 2003. Annu. Rev. Cell Dev. Biol. 19, 397–422. https://doi.org/10.1146/annurev.cellbio.19.111301.153609.

Hill, A.F., 2019. J. Neurosci. 39, 9269–9273. https://doi.org/10.1523/JNEUROSCI.0147-18.2019.

Jack, C.R., Bennett, D.A., Blennow, K., Carrillo, M.C., Feldman, H.H., Frisoni, G.B., Hampel, H., Jagust, W.J., Johnson, K.A., Knopman, D.S., Petersen, R.C., Scheltens, P., Sperling, R.A., Dubois, B., 2016. Neurology 87, 539–547. https://doi.org/10.1212/WNL.0000000000002923.

Kalluri, R., LeBleu, V.S., 2020. Science 367. https://doi.org/10.1126/science.aau6977.

Khalil, M., Teunissen, C.E., Otto, M., Piehl, F., Sormani, M.P., Gattringer, T., Barro, C., Kappos, L., Comabella, M., Fazekas, F., Petzold, A., Blennow, K., Zetterberg, H., Kuhle, J., 2018. Neurofilaments as biomarkers in neurological disorders. Nat. Rev. Neurol. 14, 577–589. https://doi.org/10.1038/s41582-018-0058-z.

Ludwig, N., Yerneni, S.S., Menshikova, E.V., Gillespie, D.G., Jackson, E.K., Whiteside, T. L., 2020. Sci. Rep. 10, 6948. https://doi.org/10.1038/s41598-020-63658-5.

Ma, W., Zhong, C., Lin, J., Chen, Z., Li, G., Tong, W., Wu, Y., Zhang, L., Lin, Z., 2022. Chin. Chem. Lett. 33, 5174–5179. https://doi.org/10.1016/j.cclet.2022.01.047.

Malm, T., Loppi, S., Kanninen, K.M., 2016. Neurochem. Int. 97, 193–199. https://doi.org/10.1016/j.neuint.2016.04.011.

Mathieu, M., Martin-Jaular, L., Lavieu, G., Théry, C., 2019. Nat. Cell Biol. 21, 9–17. https://doi.org/10.1038/s41556-018-0250-9.

Moura, S.L., Martín, C.G., Martí, M., Pividori, M.I., 2020. Talanta 211, 120657. https://doi.org/10.1016/j.talanta.2019.120657.

Orellana, A., García-González, P., Valero, S., Montrreal, L., de Rojas, I., Hernández, I., Rosende-Roca, M., Vargas, L., Tartari, J.P., Esteban-De Antonio, E., Bojaryn, U., Narvaiza, L., Alarcón-Martín, E., Alegret, M., Alcolea, D., Lleó, A., Tárraga, L., Pytel, V., Cano, A., Marquié, M., Boada, M., Ruiz, A., 2022. Int. J. Mol. Sci. 23, 6891. https://doi.org/10.3390/ijms23136891.

Patel, K.P., Wymer, D.T., Bhatia, V.K., Duara, R., Rajadhyaksha, C.D., 2020. Radiographics 40, 200–222. https://doi.org/10.1148/rg.2020190070.

Perju, A., Wongkaew, N., 2021. Anal. Bioanal. Chem. 413, 5535–5549. https://doi.org/10.1007/s00216-021-03301-y.

Pulliam, L., Sun, B., Mustapic, M., Chawla, S., Kapogiannis, D., 2019. J. Neurovirol. 25, 702–709. https://doi.org/10.1007/s13365-018-0695-4.

Radagdam, S., Khaki-Khatibi, F., Rahbarghazi, R., Shademan, B., Nourazarian, S.M., Nikanfar, M., Nourazarian, A., 2023. Front. Neurosci. 17, 1163806. https://doi.org/10.3389/fnins.2023.1163806.

Remnestål, J., Just, D., Mitsios, N., Fredolini, C., Mulder, J., Schwenk, J.M., Uhlén, M., Kultima, K., Ingelsson, M., Kilander, L., Lannfelt, L., Svenningsson, P., Nellgård, B., Zetterberg, H., Blennow, K., Nilsson, P., Häggmark-Månberg, A., 2016. Proteomics Clin. Appl. 10, 1242–1253. https://doi.org/10.1002/prca.201500150.

Rowley, P.A., Samsonov, A.A., Betthauser, T.J., Pirasteh, A., Johnson, S.C., Eisenmenger, L.B., 2020. Amyloid and tau PET imaging of alzheimer disease and other neurodegenerative conditions. Semin. Ultrasound CT MR 41, 572–583. https://doi.org/10.1053/j.sult.2020.08.011.

Sandelius, Å., Portelius, E., Källén, Å., Zetterberg, H., Rot, U., Olsson, B., Toledo, J.B., Shaw, L.M., Lee, V.M.Y., Irwin, D.J., Grossman, M., Weintraub, D., Chen-Plotkin, A., Wolk, D.A., McCluskey, L., Elman, L., Kostanjevecki, V., Vandijck, M., McBride, J., Trojanowski, J.Q., Blennow, K., 2019. Alzheimer's Dement. 15, 55–64. https://doi.org/10.1016/j.jalz.2018.08.006.

Skene, J.H., Jacobson, R.D., Snipes, G.J., McGuire, C.B., Norden, J.J., Freeman, J.A., 1986. Science 233, 783–786. https://doi.org/10.1126/science.3738509.

Soliman, H.M., Ghonaim, G.A., Gharib, S.M., Chopra, H., Farag, A.K., Hassanin, M.H., Nagah, A., Emad-Eldin, M., Hashem, N.E., Yahya, G., Emam, S.E., Hassan, A.E.A., Attia, M.S., 2021. Int. J. Mol. Sci. https://doi.org/10.3390/ijms221910794.

Srikanth, S., Woo, J.S., Gwack, Y., 2017. Small GTPases 8, 43–48. https://doi.org/10.1080/21541248.2016.1192921.

Strother, L., Miles, G.B., Holiday, A.R., Cheng, Y., Doherty, G.H., 2021. J. Neurosci. Methods 362, 109301. https://doi.org/10.1016/j.jneumeth.2021.109301.

Sweeney, M.D., Sagare, A.P., Zlokovic, B.V., 2018. Nat. Rev. Neurol. 14, 133–150. https://doi.org/10.1038/nrneurol.2017.188.

The human protein Atlas. https://www.proteinatlas.org/ENSG00000198910-L1CAM/tissue, 2024–. (Accessed 16 September 2025).

The human protein Atlas. https://www.proteinatlas.org/ENSG00000196338-NLGN3/tissue, 2024–. (Accessed 16 September 2025).

Théry, C., Witwer, K., Aikawa, E., et al., 2018. J. Extracell. Vesicles 7. https://doi.org/10.1080/20013078.2018.1535750.

Uchigashima, M., Konno, K., Demchak, E., Cheung, A., Watanabe, T., Keener, D.G., Abe, M., Le, T., Sakimura, K., Sasaoka, T., Uemura, T., Imamura Kawasawa, Y., Watanabe, M., Futai, K., 2020. eLife 9, e59545. https://doi.org/10.7554/eLife.59545.

Underwood, R., Wang, B., Carico, C., Whitaker, R.H., Placzek, W.J., Yacoubian, T.A., 2020. J. Biol. Chem. 295, 8005–8016. https://doi.org/10.1074/jbc.RA120.013337.

Valotassiou, V., Malamitsi, J., Papatriantafyllou, J., Dardiotis, E., Tsougos, I., Psimadas, D., Alexiou, S., Hadjigeorgiou, G., Georgoulias, P., 2018. Ann. Nucl. Med. 32, 583–593. https://doi.org/10.1007/s12149-018-1292-6.

Vermunt, L., Sikkes, S.A.M., van den Hout, A., Handels, R., Bos, I., van der Flier, W.M., Kern, S., Ousset, P.-J., Maruff, P., Skoog, I., Verhey, F.R.J., Freund-Levi, Y., Tsolaki, M., Wallin, Å.K., Olde Rikkert, M., Soininen, H., Spiru, L., Zetterberg, H., Blennow, K., Scheltens, P., Muniz-Terrera, G., Visser, P.J., 2019. Alzheimer disease neuroimaging initiative, AIBL research group, ICTUS/DSA study groups. Alzheimer's Dement. 15, 888–898. https://doi.org/10.1016/j.jalz.2019.04.001.

Wang, G., Dinkins, M., He, Q., Zhu, G., Poirier, C., Campbell, A., Mayer-Proschel, M., Bieberich, E., 2012. J. Biol. Chem. 287, 21384–21395. https://doi.org/10.1074/jbc.M112.340513.

Wei, R., Li, C., Fogelson, N., Li, L., 2016. Front. Aging Neurosci. 8, 76. https://doi.org/10.3389/fnagi.2016.00076.
World Medical Association, 2013. JAMA 310, 2191–2194. https://doi.org/10.1001/jama.2013.281053.
Xu, Shouying, Cao, B., Xuan, G., Xu, Shu, An, Z., Zhu, C., Li, L., Tang, C., 2024. Cell Biol. Toxicol. 40, 28. https://doi.org/10.1007/s10565-024-09866-5.
Yates, A.G., Pink, R.C., Erdbrügger, U., Siljander, P.R., Dellar, E.R., Pantazi, P., Akbar, N., Cooke, W.R., Vatish, M., Dias-Neto, E., Anthony, D.C., Couch, Y., 2022. J. Extracell. Vesicles 11. https://doi.org/10.1002/jev2.12190.
Zhang, T., Ma, S., Lv, J., Wang, X., Afewerky, H.K., Li, H., Lu, Y., 2021. Ageing Res. Rev. 68, 101321. https://doi.org/10.1016/j.arr.2021.101321.